

3D Contact and Strain in Alveolar Bone Under Tooth/Implant Loading



Yuxiao Zhou, Chujie Gong, Mehran Hossaini-Zadeh and Jing Du

Abstract In situ mechanical tester was coupled with micro-CT to investigate the effect of alveolar bone socket geometry and implant anchorage on bone–implant contact interface and the resulting strain distributions in bone. Compressive axial load was applied to occlusal surface of teeth to simulate chewing force. Then, the teeth were extracted and dental implants were placed immediately. The same compressive load was applied to bone–implant complexes. Using image processing and digital volume correlation, the displacement and strain field in the mandible bone were calculated and compared for the bone–tooth structures and bone–implant structures. Under implant loading, high strain concentration was observed in some regions in the mandible bone. In contrast, the strain distribution in bone under tooth loading was relatively uniform. The variations in the strain distribution can be attributed to the differences in the anatomies/geometries, mechanical properties and contact area with bone for implants and teeth. The clinical implications of the results are discussed for the designs of bioinspired dental implants.

Keywords Dental implant · Periodontal ligament · Digital volume correlation · Strain concentration

Y. Zhou · J. Du (✉)

Department of Mechanical and Nuclear Engineering, Penn State University,
University Park, State College, PA, USA
e-mail: jingdu@psu.edu

C. Gong

Department of Biomedical Engineering, Penn State University,
University Park, State College, PA, USA

M. Hossaini-Zadeh

Department of Oral Maxillofacial Pathology, Medicine and Surgery,
Temple University, Philadelphia, PA, USA

© The Minerals, Metals & Materials Society 2019

The Minerals, Metals & Materials Society (ed.), *TMS 2019 148th*

Annual Meeting & Exhibition Supplemental Proceedings, The Minerals,

Metals & Materials Series, https://doi.org/10.1007/978-3-030-05861-6_77

Introduction

Implant placement changes biomechanics in bone [1–3]. The biomechanics of the bone–implant construct, including mechanical strain, is related to bone–implant contact (BIC). Conventionally, BIC was measured using histology sections of bone–implant construct [4–6] and can only measure the contact area on the 2D cut surfaces. The conventional methods for strain measurement in bone and other implant-supporting materials can only measure strain on certain spots or on the surfaces of the specimens. These methods include strain gauges [7–10], photoelasticity [11], [12], Moiré interferometry [13–15], electronic speckle pattern interferometry (ESPI) [16–18], and digital image correlation (DIC) [19–22]. As a noninvasive 3D full-field method, mechanical testing coupled with micro-CT and digital volume correlation (DVC) has been applied to map strain in trabecular bone in the absence of implants [23–26]. In our prior work, we have extended this method onto the biomechanics of bone–implant constructs [27].

In this work, the contact and strain in bone–tooth and bone–implant constructs are measured and compared to reveal the change of contact and strain in bone after implant placement. In situ mechanical testing coupled with micro-CT and DVC provides an approach to noninvasively characterize 3D full-field contact and strain concurrently. The implications of results and the possible directions for future work are discussed.

Experiments and Analysis

Specimen Preparation

A fresh cadaveric mandible was obtained from National Disease Research Interchange (NDRI), approved by Institutional Review Board at Pennsylvania State University. The mandible was scanned using clinical cone beam computed tomography (CBCT) to plan the implant placement procedures. It was then cut to be a specimen containing a lateral incisor, its two adjacent teeth, and surrounding bone. The top of the lateral incisor was slightly polished to create a flat top surface for better contact in the subsequent mechanical testing. The top one-third of the crowns for the two adjacent teeth was cutoff to avoid contact in the following mechanical testing. The sectioned specimen was then partly embedded in polymethyl methacrylate (PMMA, Ortho-Jet BCA, Lang Dental, Wheeling, IL).

Following the mechanical testing on the lateral incisor, the tooth was pulled off and a dental implant (SLActive® Roxolid®, Straumann, Basel, Switzerland) with diameter of 4.1 mm and length of 10 mm was installed into the socket using a Straumann dental surgical drill kit. A conical healing abutment with diameter of 4.5 mm and height of 6.0 mm (Regular CrossFit Connection Healing Abt., Straumann, Basel, Switzerland) was installed onto the implant.

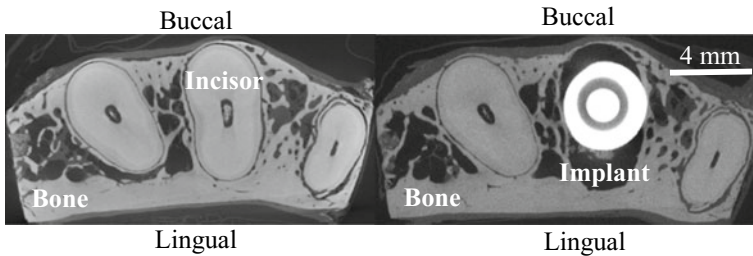


Fig. 1 Transverse slices of micro-CT images before and after implant installation

In Situ Biomechanical Testing Coupled with Micro-CT

In situ mechanical testing was performed on the lateral incisor using a static loading device (CT5000, Deben, Suffolk, UK) coupled with micro-CT (Phoenix vltomex L300 multi-scale micro-CT system, GE, Boston, MA). The specimen was first scanned under no-load condition, and then loaded at a constant displacement rate of 0.1 mm/min, until the load reached 100 N. After holding at 100 N for 1 h, the specimen was scanned at loaded condition. After implant placement, in situ mechanical testing coupled with micro-CT was also performed on the implant using the same loading protocol. Transverse cross sections of the micro-CT images with resolutions of 15 μm for the specimen before and after implant placement are presented in Fig. 1.

Contact Area Analysis

The micro-CT images were downsized, cropped and segmented in ImageJ (National Institute of Health, Maryland, USA) and Avizo 3D analysis software (FEI Visualization Sciences Group, Burlington, MA) to four parts: alveolar bone, teeth, implant and background including embedding material. The bone–tooth and bone–implant contact areas, respectively, were calculated and highlighted in red in Fig. 2. The alveolar bone was virtually sliced into distal and mesial halves to visualize the contact area in the alveolar socket.

Strain Mapping Using Digital Volume Correlation (DVC)

Digital volume correlation (DVC) analysis was performed in DaVis software (LaVision, Goettingen, Germany) on the extracted images of alveolar bone. The image stacks were divided into subvolume of pixels as correlation windows and the displacement of each correlation window was tracked by correlating the images at no-load and loaded states after fast Fourier transforms (FFT). A step-wise approach

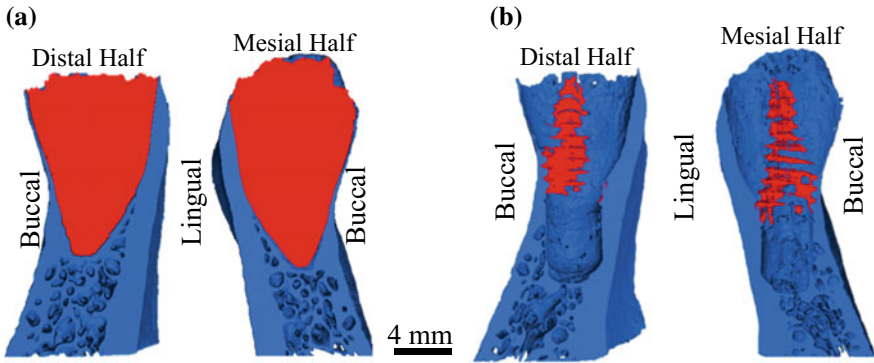


Fig. 2 a Bone–tooth contact area and b bone–implant partial contact area are highlighted in red

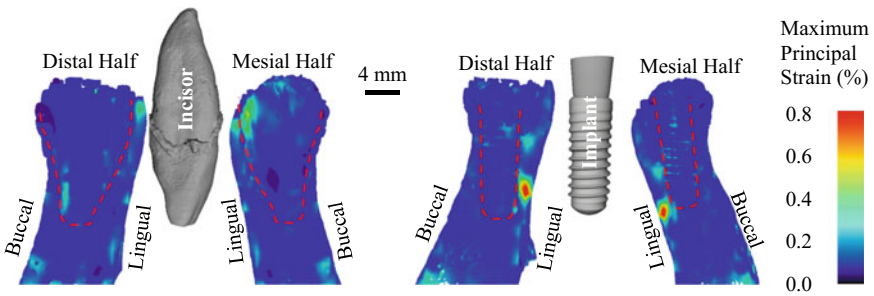


Fig. 3 Maximum principal strain on the buccal and lingual outer surfaces of the alveolar bone and inside the alveolar

was taken with the correlation window size reduced from 512 pixels to 128 and 64 pixels in each step, respectively. The overlapping ratio between adjacent correlation windows was chosen to be 50% and valid pixel threshold was set to be 50% for all steps. In post-processing, displacement vectors with correlation value below 0.5 and peak ratio below 1.5 were removed from the results and replaced by an interpolation of neighboring vectors.

The strain field obtained from DVC was visualized by rendering the results in each subvolume onto the 3D volume of alveolar bone. In Fig. 3, the distributions of maximum principal strain in alveolar bone before and after implant placement are compared. By comparing the strain mapping, a much more obvious strain concentration could be observed after implantation. Before implant placement, the strain in bone was relatively more uniform when making full contact with teeth. After the implant was placed, strain value increased and strain concentration appeared at bone–implant contact areas.

Summary

As a proof-of-concept study, in this work, we demonstrated a noninvasive method to measure the 3D bone–tooth/implant contact and 3D full-field bone strain concurrently using *in situ* mechanical testing coupled with micro-CT. The results show that the bone–tooth contact area fully covered the root of the incisor through the periodontal ligament (PDL), whereas the implant was only partly making contact with alveolar bone. Moreover, the results show that strain concentration occurred in alveolar bone after the incisor was replaced by the implant. The study paved way for future work including systematic study with larger sample size on the correlation of contact area and strain values, as well as the *in vivo* evolution of contact and strain over time. The results could provide insights on implant design and surgical planning.

Acknowledgements The project described was supported by the National Center for Advancing Translational Sciences, National Institutes of Health, through Grant UL1TR002014. The content is solely the responsibility of the authors and does not necessarily represent the official views of the NIH. The support was made available through Penn State Clinical and Translational Science Institute (CTSI). The authors are grateful to Dr. Timothy Ryan and Mr. Timothy Stecko at the Center for Quantitative Imaging (CQI) at Penn State University for technical support on micro-CT scans.

Conflict of Interest We acknowledge that all authors do not have any conflict of interest and were fully involved in the study and preparation of the manuscript.

References

1. Wazen RM, Currey JA, Guo H, Brunski JB, Helms JA, Nanci A (2013) Micromotion-induced strain fields influence early stages of repair at bone–implant interfaces. *Acta Biomater* 9(5):6663–6674
2. Brunski JB (1999) *In vivo* bone response to biomechanical loading at the bone/dental-implant interface. *Adv Dent Res* 13(1):99–119
3. Greenstein G, Cavallaro J, Tarnow D (2013) Assessing bone’s adaptive capacity around dental implants: a literature review. *J Am Dent Assoc* 144(4):362–368
4. Buser D, Schenk RK, Steinemann S, Fiorellini JP, Fox CH, Stich H (1991) Influence of surface characteristics on bone integration of titanium implants. a histomorphometric study in miniature pigs. *J Biomed Mater Res* 25(7):889–902
5. Wennerberg A, Albrektsson T, Andersson B, Krol JJ (1995) A histomorphometric and removal torque study of screw-shaped titanium implants with three different surface topographies. *Clin Oral Implants Res* 6(1):24–30
6. Jun S, Chang BMW, Weber H, Kwon J-J (2010) Comparison of initial stability parameters and histomorphometric analysis of implants inserted into extraction sockets: human fresh cadaver study. *Int J Oral Maxillofac Implants* 25(5):985–990
7. Akça K, Akkocaoglu M, Cömert A, Tekdemir I, Cehreli MC (2007) Bone strains around immediately loaded implants supporting mandibular overdentures in human cadavers. *Int J Oral Maxillofac Implants* 22(1):101–109
8. Jantarat J, Panitvisai P, Palamara JE, Messer HH (2001) Comparison of methods for measuring cuspal deformation in teeth. *J Dent* 29(1):75–82
9. Popowics TE, Rensberger JM, Herring SW (2004) Enamel microstructure and microstrain in the fracture of human and pig molar cusps. *Arch Oral Biol* 49(8):595–605

10. Asundi A, Kishen A (2000) A strain gauge and photoelastic analysis of in vivo strain and in vitro stress distribution in human dental supporting structures. *Arch Oral Biol* 45(7):543–550
11. Asundi A, Kishen A (2000) Stress distribution in the dento-alveolar system using digital photoelasticity. *Proc Inst Mech Eng H* 214(6):659–667
12. Asundi A, Kishen A (2001) Advanced digital photoelastic investigations on the tooth-bone interface. *J Biomed Opt* 6(2):224–230
13. Kishen A, Tan KBC, Asundi A (2006) Digital Moiré interferometric investigations on the deformation gradients of enamel and dentine: an insight into non-carious cervical lesions. *J Dent* 34(1):12–18
14. Wood JD, Wang R, Weiner S, Pashley DH (2003) Mapping of tooth deformation caused by moisture change using Moiré interferometry. *Dent Mater* 19(3):159–166
15. Wang RZ, Weiner S (1998) Strain-structure relations in human teeth using Moiré fringes. *J Biomech* 31(2):135–141
16. Zaslansky P, Currey JD, Friesem AA, Weiner S (2005) Phase shifting speckle interferometry for determination of strain and Young's modulus of mineralized biological materials: a study of tooth dentin compression in water. *J Biomed Opt* 10(2):024020
17. Zaslansky P, Friesem AA, Weiner S (2006) Structure and mechanical properties of the soft zone separating bulk dentin and enamel in crowns of human teeth: insight into tooth function. *J Struct Biol* 153(2):188–199
18. Zhang D, Arola DD, Rouland JA (2001) Evaluating the elastic modulus of bone using electronic speckle pattern interferometry. *Exp Tech* 25(5):32–34
19. Zhang D, Mao S, Lu C, Romberg E, Arola D (2009) Dehydration and the dynamic dimensional changes within dentin and enamel. *Dent Mater* 25(7):937–945
20. Qian L, Todo M, Morita Y, Matsushita Y, Koyano K (2009) Deformation analysis of the periodontium considering the viscoelasticity of the periodontal ligament. *Dent Mater* 25(10):1285–1292
21. Tiozzi R, Lin L, Rodrigues RCS, Heo YC, Conrad HJ, De Mattos GC, Ribeiro RF, Fok ASL (2011) Digital image correlation analysis of the load transfer by implant-supported restorations. *J Biomech* 44(6):1008–1013
22. Rossman T, Uthamaraj S, Rezaei A, McEligot S, Giambini H, Jasiuk I, Yaszemski MJ, Lu L, Dragomir-Daescu D (2017) A method to estimate cadaveric femur cortical strains during fracture testing using digital image correlation. *J Vis Exp* 127
23. Jiroušek O, Jandajsek I, Vavřík D (2011) Evaluation of strain field in microstructures using micro-CT and digital volume correlation. *J Instrum* 6(01):C01039–C01039
24. Bay BK, Smith TS, Fyhrie DP, Saad M (1999) Digital volume correlation: three-dimensional strain mapping using X-ray tomography. *Exp Mech* 39(3):217–226
25. Verhulst E, van Rietbergen B, Huiskes R (2004) A three-dimensional digital image correlation technique for strain measurements in microstructures. *J Biomech* 37(9):1313–1320
26. Zauel R, Yeni YN, Bay BK, Dong XN, Fyhrie DP (2006) Comparison of the linear finite element prediction of deformation and strain of human cancellous bone to 3D digital volume correlation measurements. *J Biomech Eng* 128(1):1–6
27. Du J, Lee J, Jang AT, Gu A, Hossaini-Zadeh M, Prevost R, Curtis DA, Ho SP (2015) Biomechanics and strain mapping in bone as related to immediately-loaded dental implants. *J Biomech*